Effects of Organic Templates on Directing the Structures of Nickel(II)−1-Hydroxyethylidenediphosphonate Compounds: A Structural and Magnetic Study

Hui-Hua Song,[†] Li-Min Zheng,*[,†] Chia-Heir Lin,[‡] Sue-Lein Wang,[‡] Xin-Quan Xin,[†] and Song Gao[§]

State Key Laboratory of Coordination Chemistry, Coordination Chemistry Institute, Nanjing University, Nanjing 210093, Department of Chemistry, National Tsing Hua University, Hsinchu, and State Key Lab of Rare Earth Materials Chemistry and Applications, Peking University, Beijing 100871, China

Received January 5, 1999. Revised Manuscript Received June 10, 1999

Hydrothermal reactions of $NiSO_4$ and 1-hydroxyethylidenediphosphonic acid ($hedpH_4$) in the presence of different organic templates resulted in the formation of three new compounds: $(enH_2)Ni(hedpH_2)_2{\cdot}2H_2O$ **1**, $(pnH_2)Ni(hedpH_2)_2(H_2O)$, **2** and $(bnH_2)Ni(hedpH_2)_2(H_2O)_2$, **3**, (hedp = 1-hydroxyethylidenediphosphonate, en = ethylenediamine, pn = 1,3-propanediamine, bn = 1,4-butylenediamine). Crystal data: **1**, monoclinic, *C*2/*c*, a = 24.7864(5), b = 5.2565(1), c = 16.0468(2) Å, β = 117.903(1)°, V = 1847.67(6) Å^3, Z = 4; **2**, triclinic, $P\bar{1}$, a = 10.0926(4), b = 10.5621(4), c = 10.9212(4) Å, α = 111.520(1), β = 110.833(1), γ = 93.630(1)°, V = 986.77(7) Å^3, Z = 2; **3**, monoclinic, *C*2/*c*, a = 16.230(2), b = 12.430(13), c = 12.657(13) Å, β = 121.997(10)°, V = 2165(4) Å^3, Z = 4. The compound **1** has a one-dimensional chain structure which is composed of corner-sharing $\{NiO_6\}$ octahedra and $\{O_3PC\}$ tetrahedra with the ethylenediammonium cations and water molecules stabilized between the chains. By replacing ethylenediamine with 1,3-propanediamine or 1,4-butylenediamine, molecular species have been obtained. The compound **2** contains dimers of $[Ni(hedpH_2)_2(H_2O)]_2^{2-}$ whereas **3** is a mononuclear compound. The thermal stabilities, spectroscopic and magnetic properties of all three compounds have been investigated.

Introduction

During the past decade, a rapid expansion has been witnessed on the research of metal phosphonates because of their potential applications in the areas of sorption and ion exchange, catalysis, and sensors.[1−3] Work in this area was originally concentrated on the phosphonates of group IV metals,[4,5] and then extended to the divalent or trivalent metals.[6−13] To our knowledge, reports in terms of nickel phosphonates are rather few. So far only a handful of examples of nickel monophosphonates with formula $Ni(O_3PR){\cdot}H_2O$ have been described,[8,9,13] which were supposed to be isostructural to the Mn and Mg analogues. No single-crystal structures of nickel phosphonates have yet been determined.

In most cases, the metal phosphonate compounds exhibit layered structures with the metal atoms bridged by oxygen atoms. The organic moieties of the phosphonates project into the interlayer space. With regard to metal diphosphonates $[M{-}R'(PO_3)_2^{4-}]$, crystal engineering of one- to three-dimensional structures could be accomplished by changing the reaction conditions, the length, and structure of diphosphonate tether R′ and by introducing different templates, etc. The influences of these variations have been interpreted by Zubieta and Haushalter et al.[14−16] in synthesizing a series of compounds of $V{-}O{-}RPO_3^{2-}/R'(PO_3)_2^{4-}$ system. The template effects on the construction of nickel phosphonates

* To whom correspondence should be addressed. E-mail: lmzheng@netra.nju.edu.cn. Fax: +86-25-3314502.
† Nanjing University.
‡ Tsing Hua University.
§ Peking University.

(1) Clearfield, A. In *New Developments in Ion Exchange Materials*; Abe, M., Kataoka, T., Suzuki, T., Eds.; Kodansha, Ltd.: Tokyo, 1991.
(2) Cao, G.; Hong, H.-G.; Mallouk, T. E. *Acc. Chem. Res.* **1992**, *25*, 420.
(3) Vermeulen, L. A. Molecular Level Artificial Photosynthetic Materials. *Progress in Inorganic Chemistry*; Meyer, G. J., Ed.; 1997; Vol. 44, p 143.
(4) Clearfield, A.; Costantino, U. In *Comprehensive Supramolecular Chemistry*, Alberti, G., Bein, T., Eds.; Pergamon Press: Oxford, 1996; Vol. 7, p 107.
(5) Dines, M. B.; DiGiacomo, P. M. *Inorg. Chem.* **1981**, *20*, 92.
(6) Frink, F. J.; Wang, R.-C.; Colon, J. L.; Clearfield, A. *Inorg. Chem.* **1991**, *30*, 1438.
(7) Ortiz-Avila, Y.; Rudolf, P. R.; Clearfield, A. *Inorg. Chem.* **1989**, *28*, 2137.
(8) Martin, K.; Squattrino, P. J.; Clearfield, A. *Inorg. Chim. Acta* **1989**, *155*, 7.
(9) Cunningham, D.; Hennelly, P. J. D. *Inorg. Chim. Acta* **1979**, *37*, 95.
(10) Poojary, D. M.; Zhang B.; Bellinghausen, P.; Clearfield, A. *Inorg. Chem.* **1996**, *35*, 5254.
(11) Drumel, S.; Janvier, P.; Barboux, P.; Bujoli-Doeuff, M.; Bujoli, B. *Inorg. Chem.* **1995**, *34*, 148.
(12) Lohse, D. L.; Sevov, S. C. *Angew. Chem., Int. Ed. Engl.* **1997**, *36*, 1619.
(13) Hix, G. B.; Harris, K. D. M. *J. Mater. Chem.* **1998**, *8*, 579.
(14) Khan, M. I.; Lee, Y.-S.; O'Connor, C. J.; Haushalter, R. C.; Zubieta, J. *J. Am. Chem. Soc.* **1994**, *116*, 4525.
(15) Soghomonian, V.; Diaz, R.; Haushalter, R. C.; O'Connor, C. J.; Zubieta, J. *Inorg. Chem.* **1995**, *34*, 4460.
(16) Soghomonian, V.; Chen, Q.; Haushalter, R. C.; Zubieta, J. *Angew. Chem., Int. Ed.* Engl. **1995**, *34*, 223.

10.1021/cm990011v CCC: $18.00
Published on Web 08/11/1999

remain unexplored. Herein the influence of organic diamines on directing the formation of Ni−hedp (hedp = 1-hydroxyethylidenediphosphonate) compounds has been studied.

It is worth noting that the metal−hedp complexes which have been structurally determined are still limited. Zapf et al.[17] synthesized a Sn(II) compound [Sn_2(hedp)], showing a three-dimensional open framework structure. A mixed-valence copper(I/II) compound $Na_2Cu_{15}(hedp)_6(OH)_2(H_2O)$ with an interesting framework structure was recently reported by us.[18] When hedp is partially protonated, lower dimensional compounds can be achieved. Nash et al.[19] described the structures of several one-dimensional lanthanide−hedpH_n ($n = 1-3$) complexes which were prepared in solution at room temperature. Polynuclear compounds with metal ions such as Mo have also been reported.[20] In this paper, we describe the hydrothermal syntheses and characterizations of three new compounds, including $(enH_2)Ni(hedpH_2)_2{\cdot}2H_2O$ **1**, $(pnH_2)Ni(hedpH_2)_2(H_2O)$, **2**, and $(bnH_2)Ni(hedpH_2)_2(H_2O)_2$, **3**, (en = ethylenediamine, pn = 1,3-propanediamine, bn = 1,4-butylenediamine).

Experimental Section

Materials and Methods. All the starting materials were reagent grade and used as purchased. The elemental analyses were performed on a PE 240C elemental analyzer. The infrared spectra were recorded on IFS66V spectrometer with pressed KBr pellets. The diffuse reflectance UV−vis spectra were carried out on a Shimadzu UV-240 spectrometer. Thermal analyses were performed in nitrogen with a heating rate of 5 °C/min on a TGA-DTA V1.1B TA Inst 2100 instrument. Variable-temperature magnetic susceptibility data were obtained on a polycrystalline sample (54.8 mg for **1**, 100 mg for **2**, and 42.9 mg for **3**) from 2 to ∼280 K in a magnetic field of 10 kG after zero-field cooling using a MagLab System 2000 magnetometer. Diamagnetic corrections were estimated from Pascal's constants.[21]

Synthesis of $(enH_2)Ni(hedpH_2)_2{\cdot}2H_2O$, 1. The compound was prepared by heating a mixture of $NiSO_4{\cdot}7H_2O$ (1 mmol, 0.2814 g), 50% hedpH_4 (1 cm^3), LiF (1 mmol, 0.0255 g), and H_2O (8 cm^3), adjusted to pH = 3 by ethylenediamine, in a Teflon-lined stainless autoclave at 140 °C for 48 h. After the mixture was slowly cooled to room temperature, pale yellow needles were discovered which are monophasic as judged by comparison of the powder X-ray diffraction of the bulk product with the pattern simulated from the single-crystal study. The products were used for both the single-crystal structural determination and the physical properties measurements. Found: C, 12.42; H, 4.68; N, 4.42. Calcd: C, 12.75; H, 4.60; N, 4.96%. IR (KBr): 3565m, 3151s (br), 1638m, 1539m, 1490w, 1416m, 1345w, 1151s, 1081s, 1042s, 928s, 908s, 813m, 725m, 645m, 561s, 489w, 464w cm^{-1}.

Synthesis of $(pnH_2)Ni(hedpH_2)_2(H_2O)$, 2. A mixture of $NiSO_4{\cdot}7H_2O$ (0.9 mmol, 0.2486 g), 50% hedpH_4 (1 cm^3), LiF (1 mmol, 0.0264 g), and H_2O (8 cm^3) was adjusted by 1,3-propanediamine to pH = 3. The mixture was transferred to a Teflon-lined stainless autoclave and heated at 140 °C for 72 h. After the mixture was cooled to room temperature, pale yellow crystals were recovered as a monophase, judged by the powder X-ray diffraction pattern. The crystals were used for single-crystal structural determination and the physical properties measurements. Found: C, 15.16; H, 5.37; N, 5.39. Calcd: C, 14.98; H, 4.64; N, 4.99%. IR (KBr): 3608m, 3275s(br), 1623m, 1525m, 1506m, 1397m, 1371w, 1237s, 1182s, 1133s, 1067s, 1026s, 938s, 914s, 818m, 762w, 647m, 549s, 503m, 472m, 445m cm^{-1}.

Synthesis of $(bnH_2)Ni(hedpH_2)_2(H_2O)_2$, 3. The hydrothermal treatment of a mixture of $NiSO_4{\cdot}7H_2O$ (1 mmol, 0.2846 g), 50% hedpH_4 (1 cm^3), LiF (1 mmol, 0.0252 g), and H_2O (8 cm^3), adjusted by 1,4-butylenediamine to pH = 3, at 140 °C for 48 h led to the formation of monophasic compound **3**, as proved by the powder X-ray diffraction pattern. The green crystals were used for both single-crystal structural determination and the physical properties measurements. Found: C, 15.99; H, 4.58; N, 4.44. Calc.: C, 16.20; H, 5.06; N, 4.72%. IR (KBr): 3564m, 3280s(br), 1640m, 1507m, 1469m, 1449w, 1401m, 1374w, 1278m, 1161s, 1140s, 1122s, 1026s, 956s, 928s, 815m, 741w, 647m, 560s, 523m, 505m, 470s, 457s cm^{-1}.

The effects of pH and the metal ligand ratio on the products have been studied. The increase of pH (4−6) led to the formation of unidentified yellow powders in all three cases. By maintaining the pH at 3, the increase of metal ligand ratio (2 or 3 mmol:1 mL) resulted in the same monophase of **1**, but mixtures with unidentified yellow-green or green powder impurities in the cases of **2** and **3**.

Crystallographic Studies. Single crystals of dimensions 0.25 × 0.05 × 0.02 mm for **1**, 0.3 × 0.1 × 0.1 mm for **2** and 0.25 × 0.1 × 0.1 for **3** were used for structural determinations on a Siemens Smart-CCD diffractometer equipped with a normal focus, 3 kW sealed tube X-ray source and graphite-monochromated Mo Kα radiation (λ = 0.71073 Å) at room temperature. Intensity data were collected in 1271 frames for all three compounds with increasing ω (width of 0.30° per frame). Number of measured and observed reflections [$I > 2\sigma(I)$]: 5205, 2085 (R_{int} = 0.0247) for **1**; 9480, 4251 (R_{int} = 0.0287) for **2**; and 6226, 2352 (R_{int} = 0.0287) for **3**. Empirical absorption corrections were applied using the SADABS program for Siemens area detector ($T_{min,max}$: 0.821, 0.962 for **1**; 0.733, 0.973 for **2**; and 0.808, 0.988 for **3**). The extinction corrections were applied for **2** and **3**, with the extinction coefficient 0.0024(6) for **2** and 0.0008(2) for **3**, respectively.

The structures were solved by direct methods and refined on F^2 by full-matrix least squares using SHELXTL.[22] All non-hydrogen atoms were refined with anisotropic displacement parameters. The ammonium cations in **2** and **3** are disordered. All hydrogen atoms were located in difference electron density maps and refined with fixed isotropic displacement parameters. Crystallographic data are summarized in Table 1, atomic coordinates in Tables 2−4, and selected bond lengths and angles in Tables 5−7.

Results and Discussion

Thermal Analysis and Spectroscopic Studies. The thermal analyses of compounds **1**−**3** have been performed in the temperature range 30−600 °C. The compound **1** is thermally stable until about 240 °C. Between 240 and 318 °C, it decomposes in approximately two steps with a total weight loss of 17.35%. This value corresponds to the release of two water molecules and one ethylenediamine molecule (calcd 16.99%). Compounds **2** and **3** start to decompose at 170 °C and 140 °C, respectively. The assignments of the weight loss between 140 and 350 °C are listed in Table 8. The results are in agreement with the formula of **1**−**3**. The further weight losses immediately after the release of organic amines in all three cases suggest the collapse of the crystal lattice. The weight loss above 360 °C could

(17) Zapf, P. J.; Rose, D. J.; Haushalter, R. C.; Zubieta, J. *J. Solid State Chem*. **1996**, *125*, 182.

(18) Zheng, L.-M.; Duan, C.-Y.; Ye, X.-R.; Zhang, L.-Y.; Wang, C.; Xin, X.-Q. *J. Chem. Soc., Dalton Trans*. **1998**, 905.

(19) Nash, K. L.; Rogers, R. D.; Ferraro, J.; Zhang, J. *Inorg. Chim. Acta* **1998**, *269*, 211.

(20) Krol', I. A.; Starikova, Z. A.; Sergienko, V. S.; Tolkacheva, E. O. *Russ. J. Inorg. Chem*. **1991**, *36* (2), 226, and references therein.

(21) Kahn, O. *Molecular Magnetism*; VCH Publishers: New York, 1993.

(22) Sheldrick, G. M. *SHELXTL PC*, version 5; Siemens Analytical X-ray Instruments Inc.: Madison, WI, 1995.

Table 1. Crystallographic Data

compound	**1**	**2**	**3**
formula	$C_6H_{26}N_2NiO_{16}P_4$	$C_7H_{26}N_2NiO_{15}P_4$	$C_8H_{30}N_2NiO_{16}P_4$
M	564.88	560.89	592.93
crystal system	monoclinic	triclinic	monoclinic
space group	*C*2/*c*	$P\bar{1}$	*C*2/*c*
a,Å	24.7864(5)	10.0926(4)	16.227(17)
b,Å	5.2565(1)	10.5621(4)	12.430(13)
c,Å	16.0468(2)	10.9212(4)	12.657(13)
α, deg		111.520(1)	
β, deg	117.903(1)	110.833(1)	121.997(10)
γ,deg		93.630(1)	
V, Å^3	1847.67(6)	986.77(7)	2165(4)
Z	4	2	4
D_c, g cm^{-3}	2.031	1.888	1.819
F(000)	1168	580	1232
μ(Mo Kα), cm^{-1}	14.84	13.85	12.71
goodness of fit on F^2	1.101	1.103	1.098
*R*1, *wR*2[a] [$I > 2\sigma(I)$]	0.0290, 0.0649	0.0287, 0.0684	0.0314, 0.0710
(all data)	0.0398, 0.0704	0.0336, 0.0722	0.0370, 0.0747
$(\Delta\rho)_{max}$, $(\Delta\rho)_{min}$/e Å^{-3}	0.379, −0.355	0.454, −0.324	0.775, −0.746

[a] $R_1 = \sum||F_o| - |F_c||/\sum|F_o|$. $wR_2 = [\sum w(F_o^2 - F_c^2)^2/\sum w(F_o^2)^2]^{1/2}$.

Table 2. Atomic Coordinates (×10^4) and Equivalent Isotropic Displacement Parameters (Å^2 × 10^3) for 1

atom	*x*	*y*	*z*	*U*(eq)[a]
Ni(1)	0	0	0	10(1)
P(1)	618(1)	4936(1)	1458(1)	11(1)
P(2)	−1244(1)	−2943(1)	−332(1)	12(1)
O(1)	105(1)	3129(3)	876(1)	14(1)
O(2)	548(1)	−2318(3)	1163(1)	15(1)
O(3)	738(1)	4952(4)	2512(1)	21(1)
O(4)	−749(1)	−977(3)	128(1)	15(1)
O(5)	−1857(1)	−2234(3)	−425(1)	18(1)
O(6)	−1067(1)	−5539(3)	213(1)	20(1)
O(7)	1449(1)	1217(3)	2027(1)	18(1)
O(1W)	727(1)	386(5)	3182(2)	37(1)
N(1)	2097(1)	10083(4)	4043(2)	21(1)
C(1)	1323(1)	3603(4)	1514(2)	14(1)
C(2)	2293(1)	12638(5)	4475(2)	22(1)
C(3)	1866(1)	5346(5)	2066(2)	20(1)

[a] *U*(eq) is defined as one-third of the trace of the orthogonalized U_{ij} tensor

be due to the decomposition of organophosphonate groups for all three compounds.

The infrared spectra of **1**−**3** exhibited a series of bands in the 1000−1200 cm^{-1} range associated with PO_3 group vibrations. The broad band appeared around 3200 cm^{-1} is due to O−H stretchings of hydrogen-bonded hydroxyl groups including water molecules, the α-hydroxy group and protonated phosphonates.[19]

The diffuse reflectance spectra for **1**−**3** feature the octahedral geometry around the nickel atoms. The bands at ∼13 000 cm^{-1} and ∼24 000 cm^{-1} are assigned to the $^3T_{1g} \leftarrow {}^3A_{2g}$ and $^3T_{1g}(P) \leftarrow {}^3A_{2g}$ transitions, respectively. The shoulder peaks at ∼15 000 cm^{-1} and ∼21 000 cm^{-1} are assigned to the spin inhibited transitions of $^1E_g \leftarrow {}^3A_{2g}$ and $^1T_{1g} \leftarrow {}^3A_{2g}$ transitions (Table 9).[9]

Description of the Structure 1. As shown in Figures 1 and 2, the structure of the compound **1** consists of one-dimensional chains of corner-sharing $\{NiO_6\}$ octahedra and $\{O_3PC\}$ tetrahedra, with the enH_2^{2+} cations and water molecules present between the chains. The Ni atom sits on an inversion center. The coordination geometry of each nickel atom is defined by

Table 3. Atomic Coordinates (×10^4) and Equivalent Isotropic Displacement Parameters (Å^2 × 10^3) for 2

atom	*x*	*y*	*z*	*U*(eq)[a]
Ni(1)	3302(1)	5706(1)	8145(1)	17(1)
P(1)	2799(1)	6564(1)	5389(1)	17(1)
P(2)	1066(1)	7588(1)	7220(1)	17(1)
P(3)	6598(1)	7695(1)	9959(1)	20(1)
P(4)	6262(1)	4534(1)	8708(1)	17(1)
O(1)	3404(2)	5758(2)	6281(2)	21(1)
O(2)	3843(2)	7112(2)	4900(2)	25(1)
O(3)	1367(2)	5672(2)	4034(2)	23(1)
O(4)	1908(2)	7048(2)	8293(2)	22(1)
O(5)	−321(2)	6595(2)	6000(2)	23(1)
O(6)	622(2)	8958(2)	7971(2)	26(1)
O(7)	4958(2)	7472(2)	9386(2)	24(1)
O(8)	7351(2)	8998(2)	10013(2)	30(1)
O(9)	7242(2)	7742(2)	11525(2)	36(1)
O(10)	4624(2)	4280(2)	7941(2)	22(1)
O(11)	6826(2)	3367(2)	7764(2)	26(1)
O(12)	6857(2)	4569(2)	10180(2)	31(1)
O(13)	3643(2)	8949(2)	7710(2)	26(1)
O(14)	6471(2)	6161(2)	7365(2)	25(1)
O(15)	1579(2)	3966(2)	6849(2)	25(1)
N(1)	3294(2)	2751(2)	4661(2)	32(1)
N(2)	3497(3)	−974(3)	1238(2)	37(1)
C(1)	2303(2)	8077(2)	6491(2)	19(1)
C(2)	1685(3)	8936(3)	5655(3)	31(1)
C(3)	7065(2)	6198(2)	8801(2)	20(1)
C(4)	8720(3)	6409(3)	9303(3)	30(1)
C(5)	2728(3)	1321(3)	4442(3)	31(1)
C(6)	2405(4)	263(4)	2882(5)	28(1)
C(6′)	3432(10)	269(8)	3643(10)	35(3)
C(7)	3778(4)	−153(4)	2762(4)	23(1)
C(7′)	2601(11)	−221(10)	2053(10)	42(3)

[a] *U*(eq) is defined as one-third of the trace of the orthogonalized U_{ij} tensor

Table 4. Atomic Coordinates (×10^4) and Equivalent Isotropic Displacement Parameters (Å^2 × 10^3) for 3

atom	*x*	*y*	*z*	*U*(eq)[a]
Ni(1)	0	7249(1)	2500	17(1)
P(1)	−1511(1)	5356(1)	648(1)	17(1)
P(2)	2059(1)	6684(1)	2766(1)	17(1)
O(1)	−635(1)	6090(1)	1137(1)	21(1)
O(2)	−2401(1)	5848(1)	−565(2)	23(1)
O(3)	−1350(1)	4225(1)	3762)	25(1)
O(4)	2877(1)	7239(1)	3907(2)	23(1)
O(5)	1091(1)	7263(1)	2131(2)	21(1)
O(6)	2419(1)	6526(2)	1852(2)	25(1)
O(7)	−1060(1)	4853(1)	2947(2)	25(1)
O(1W)	−701(1)	8481(2)	1204(2)	25(1)
N(1)	158(2)	2882(2)	593(2)	35(1)
C(1)	−1861(2)	5327(2)	1818(2)	19(1)
C(2)	−2737(2)	4596(2)	1392(3)	29(1)
C(3)	−157(3)	1888(3)	870(4)	65(1)
C(4)	235(5)	2293(7)	2422(7)	53(2)
C(5)	68(8)	1509(6)	1960(7)	71(3)

[a] *U*(eq) is defined as one-third of the trace of the orthogonalized U_{ij} tensor

six O atoms from four $hedpH_2^{2-}$ anions. The Ni−O bond distances fall in the range 2.028(2)−2.107(2) Å. The two $hedpH_2^{2-}$ ligands are tridentate and symmetrically equivalent. Each $hedpH_2^{2-}$ chelates to the Ni atom through O1 and O4A atoms from its two $\{PO_3H\}$ moieties. The $\{P(1)O_3H\}$ terminus further bridges the neighboring nickel atoms through the coordination of the atom O2 to form infinite chains along the *b* direction. Both O3 and O6 in the diphosphonate ligand are protonated. The P−O(H) bond lengths [1.573(2), 1.569(2) Å] are distinctly longer than those of P═O [1.504(2) Å] and P−O(Ni) [1.504(2)−1.510(2) Å]. The coordination mode of $hedpH_2^{2-}$ in compound **1** is reminiscent

Table 5. Bond Lengths [Å] and Angles [deg] for 1[a]

Ni(1)−O(4)	2.028(2) 2×	Ni(1)−O(1)	2.099(2) 2×
Ni(1)−O(2)	2.107(2) 2×	P(1)−O(1)	1.510(2)
P(1)−O(2B)	1.504(2) 2×	P(1)−O(3)	1.573(2)
P(1)−C(1)	1.848(2)	P(2)−O(4)	1.507(2)
P(2)−O(5)	1.504(2)	P(2)−O(6)	1.569(2)
P(2)−C(1A)	1.845(2) 2×	O(7)−C(1)	1.452(3)
N(1)−C(2)	1.485(3)	C(1)−C(3)	1.523(3)
C(2)−C(2D)	1.514(5)		
O(1A)−Ni(1)−O(1)	180.0 3×	O(4)−Ni(1)−O(1)	87.89(6) 2×
O(4)−Ni(1)−O(1A)	92.11(6) 2×	O(4A)−Ni(1)−O(2)	89.67(6) 2×
O(4)−Ni(1)−O(2)	90.33(6) 2×	O(1)−Ni(1)−O(2)	91.94(6) 2×
O(1A)−Ni(1)−O(2)	88.06(6) 2×	O(2B)−P(1)−O(1)	118.04(9)
O(2B)−P(1)−O(3)	105.68(10)	O(1)−P(1)−O(3)	110.48(10)
O(2B)−P(1)−C(1)	110.18(10)	O(1)−P(1)−C(1)	107.13(9)
O(3)−P(1)−C(1)	104.56(10)	O(5)−P(2)−O(4)	115.61(9)
O(5)−P(2)−O(6)	106.09(10)	O(4)−P(2)−O(6)	111.84(10)
O(5)−P(2)−C(1A)	109.17(10)	O(4)−P(2)−C(1A)	107.66(9)
O(6)−P(2)−C(1A)	106.07(10)	P(1)−O(1)−Ni(1)	135.43(9)
P(1C)−O(2)−Ni(1)	139.94(10)	P(2)−O(4)−Ni(1)	134.29(10)
O(7)−C(1)−C(3)	107.0(2)	O(7)−C(1)−P(2A)	108.19(14)
C(3)−C(1)−P(2A)	110.6(2)	O(7)−C(1)−P(1)	107.60(14)
C(3)−C(1)−P(1)	111.0(2)	P(2A)−C(1)−P(1)	112.26(11)
N(1)−C(2)−C(2D)	109.6(3)		

[a] Symmetry transformations used to generate equivalent atoms: A, $-x, -y, -z$; B, $x, y+1, z$; C, $x, y-1, z$; D, $-x+{}^1/_2, -y+{}^5/_2, -z+1$.

Table 6. Bond Lengths [Å] and Angles [deg] for 2[a]

Ni(1)−O(12A)	2.012(2)	Ni(1)−O(7)	2.061(2)
Ni(1)−O(4)	2.064(2)	Ni(1)−O(10)	2.079(2)
Ni(1)−O(1w)	2.084(2)	Ni(1)−O(1)	2.096(2)
P(1)−O(2)	1.510(2)	P(1)−O(1)	1.514(2)
P(1)−O(3)	1.565(2)	P(1)−C(4)	1.836(2)
P(2)−O(4)	1.505(2)	P(2)−O(5)	1.516(2)
P(2)−O(6)	1.562(2)	P(2)−C(4)	1.840(2)
P(3)−O(8)	1.501(2)	P(3)−O(7)	1.514(2)
P(3)−O(9)	1.579(2)	P(3)−C(6)	1.837(2)
P(4)−O(12)	1.488(2)	P(4)−O(10)	1.516(2)
P(4)−O(11)	1.575(2)	P(4)−C(6)	1.840(2)
O(13)−C(1)	1.454(3)	O(14)−C(3)	1.451(3)
C(1)−C(2)	1.522(3)	C(3)−C(4)	1.534(3)
O(12A) −Ni(1)−O(7)	95.51(7)	O(12A)−Ni(1)−O(4)	88.78(7)
O(7)−Ni(1)−O(4)	86.04(6)	O(12A)−Ni(1)−O(10)	90.92(7)
O(7)−Ni(1)−O(10)	96.54(6)	O(4)−Ni(1)−O(10)	177.42(6)
O(12A)−Ni(1)−O(1w)	85.83(7)	O(7)−Ni(1)−O(1w)	177.70(7)
O(4)−Ni(1)−O(1w)	92.13(7)	O(10)−Ni(1)−O(1w)	85.30(6)
O(12A)−Ni(1)−O(1)	173.83(7)	O(7)−Ni(1)−O(1)	89.67(6)
O(4)−Ni(1)−O(1)	94.92(6)	O(10)−Ni(1)−O(1)	85.16(6)
O(1w)−Ni(1)−O(1)	89.10(6)	O(2)−P(1)−O(1)	114.76(10)
O(2)−P(1)−O(3)	108.56(9)	O(1)−P(1)−O(3)	111.41(9)
O(2)−P(1)−C(1)	107.26(10)	O(1)−P(1)−C(1)	108.13(9)
O(3)−P(1)−C(1)	106.31(10)	O(4)−P(2)−O(5)	115.68(9)
O(4)−P(2)−O(6)	111.22(9)	O(5)−P(2)−O(6)	106.36(9)
O(4)−P(2)−C(1)	107.13(10)	O(5)−P(2)−C(1)	110.12(10)
O(6)−P(2)−C(1)	105.93(10)	O(8)−P(3)−O(7)	114.35(10)
O(8)−P(3)−O(9)	108.13(11)	O(7)−P(3)−O(9)	110.39(11)
O(8)−P(3)−C(3)	108.05(10)	O(7)−P(3)−C(3)	108.57(10)
O(9)−P(3)−C(3)	107.08(10)	O(12)−P(4)−O(10)	117.49(10)
O(12)−P(4)−O(11)	106.87(10)	O(10)−P(4)−O(11)	109.16(9)
O(12)−P(4)−C(3)	108.69(11)	O(10)−P(4)−C(3)	107.67(10)
O(11)−P(4)−C(3)	106.45(10)	P(1)−O(1)−Ni(1)	134.15(9)
P(2)−O(4)−Ni(1)	129.62(9)	P(3)−O(7)−Ni(1)	132.76(10)
P(4)−O(10)−Ni(1)	128.66(9)	P(4)−O(12)−Ni(1A)	154.10(12)
O(13)−C(1)−C(2)	107.5(2)	O(13)−C(1)−P(1)	106.52(14)
C(2)−C(1)−P(1)	110.8(2)	O(13)−C(1)−P(2)	107.32(14)
C(2)−C(1)−P(2)	111.6(2)	P(1)−C(1)−P(2)	112.73(11)
O(14)−C(3)−C(4)	107.6(2)	O(14)−C(3)−P(3)	106.79(14)
C(4)−C(3)−P(3)	110.4(2)	O(14)−C(3)−P(4)	108.40(14)
C(4)−C(3)−P(4)	111.3(2)	P(3)−C(3)−P(4)	112.16(12)

[a] Symmetry transformations used to generate equivalent atoms: A, $-x+1, -y+1, -z+2$.

of those in $Ln(hedpH_3)(hedpH_2)\cdot 5H_2O$[19] and the $(HO_3PCH_2PO_3H)^{2-}$ group in chain compound $[Sn(HO_3PCH_2PO_3H)]\cdot H_2O$.[17]

Between the chains, there exists extensive H-bondings which hold the water molecules and hydrated ethylenediamine cations in crystal lattice [O3···O1w, 2.635(3); O7···O1w, 3.152(4); N1···O5 (1), 2.825(4); N1···O1w[i], 3.011(4); N1···O7[i], 2.922(3); N1···O5[ii], 2.761(3); O7···O4[iii], 3.061(2); O1w···O3[iv], 3.057(3); O6···O4[iv], 2.985(2); O6···O1[iv], 2.677(3); O1w···O4[v], 2.780(4) Å].[23] The strong hydrogen bondings are responsible for the higher removal temperature of lattice water in **1**.

Table 7. Bond Lengths [Å] and Angles [deg] for 3[a]

Ni(1)−O(5)	2.056(2) 2×	Ni(1)−O(1)	2.056(2) 2×
Ni(1)−O(1W)	2.087(2) 2×	P(1)−O(1)	1.518(2)
P(1)−O(2)	1.571(2)	P(1)−O(3)	1.502(2)
P(1)−C(1)	1.845(3)	P(2)−O(4)	1.514(2)
P(2)−O(5)	1.514(2)	P(2)−O(6)	1.561(2)
P(2)−C(1A)	1.845(3)	O(7)−C(1)	1.453(3)
C(1)−C(2)	1.525(4)		
O(5)−Ni(1)−O(5A)	179.06(9)	O(5)−Ni(1)−O(1)	85.68(8) 2×
O(5A)−Ni(1)−O(1)	94.98(8) 2×	O(1)−Ni(1)−O(1A)	91.08(12)
O(5)−Ni(1)−O(1W)	89.51(9) 2×	O(5A)−Ni(1)−O(1W)	89.80(9) 2×
O(1)−Ni(1)−O(1W)	91.85(11) 2×	O(1A)−Ni(1)−O(1W)	174.81(7) 2×
O(1W)−Ni(1)−O(1WA)	85.55(13)	O(1)−P(1)−O(2)	109.95(11)
O(3)−P(1)−O(1)	114.67(12)	O(3)−P(1)−O(2)	108.76(11)
O(1)−P(1)−C(1)	107.71(11)	O(2)−P(1)−C(1)	106.08(13)
O(3)−P(1)−C(1)	109.32(11)	O(4)−P(2)−O(6)	106.29(13)
O(5)−P(2)−O(4)	115.36(11)	O(5)−P(2)−O(6)	110.92(12)
O(5)−P(2)−C(1A)	107.32(11)	O(4)−P(2)−C(1A)	109.98(11)
O(6)−P(2)−C(1A)	106.67(11)	P(1)−O(1)−Ni(1)	135.09(10)
P(2)−O(5)−Ni(1)	130.63(12)	O(7)−C(1)−C(2)	106.7(2)
O(7)−C(1)−P(1)	107.6(2)	C(2)−C(1)−P(1)	110.7(2)
O(7)−C(1)−P(2A)	106.9(2)	C(2)−C(1)−P(2A)	112.0(2)
P(1)−C(1)−P(2A)	112.66(12)		

[a] Symmetry transformations used to generate equivalent atoms: A, $-x, y, -z+{}^1/_2$.

Table 8. Assignment of the Thermogravimetric Analyses for 1−3

		wt loss, %	
compound	*T* range, °C	observed	calculated
1	240−318	17.35	16.99 ($-2H_2O$-en)
2	170−250	3.34	3.21 ($-H_2O$)
	290−330	13.20	13.19 (−pn)
3	140−218	7.91	6.07 ($-2H_2O$)

Table 9. Assignment of the Diffuse Reflectance Spectra for 1−3

compds	*a*	*b*	*c*	*d*	*e*
1	−	12 563	14 881	20 576	24 038
2	−	13 089	14 793	21 008	24 155
3	−	13 441	15 106	21 277	25 000

[a] $^3T_{2g} \leftarrow {}^3A_{2g}$. [b] $^3T_{1g} \leftarrow {}^3A_{2g}$. [c] $^1E_g \leftarrow {}^3A_{2g}$. [d] $^1T_{1g} \leftarrow {}^3A_{2g}$. [e] $^3T_{1g}(P) \leftarrow {}^3A_{2g}$.

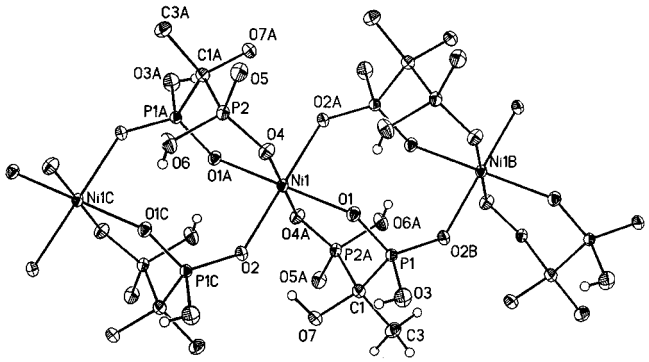

Figure 1. A fragment of the chain with atomic labeling scheme (50% probability) in **1**.

(23) Symmetry code: (i) $x, y+1, z$; (ii) $x+{}^1/_2, -y+{}^1/_2, z+{}^1/_2$. (iii) $-x, -y, -z$; (iv) $x, y-1, z$; (v) $x, y, -z+{}^1/_2$.

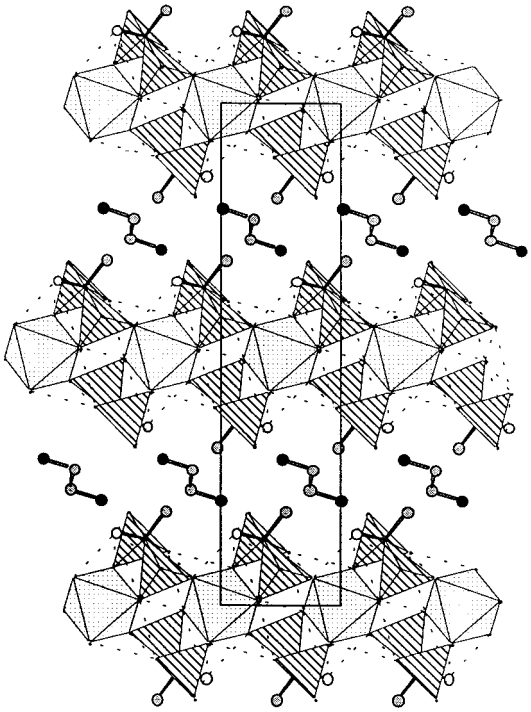

Figure 2. Polyhedral representation of the structure of **1** packed along *c* axis. All the H atoms and N···hydrogen bondings are omitted for clarity.

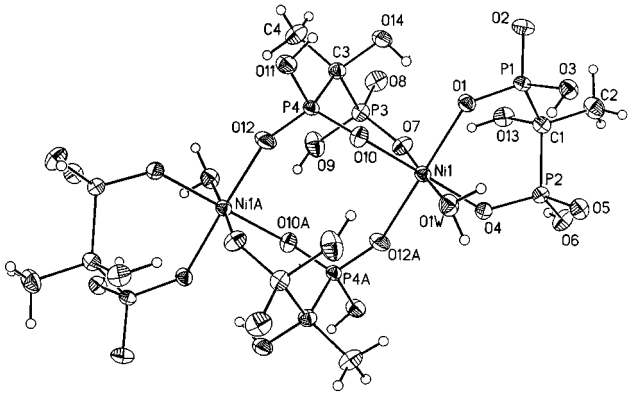

Figure 3. The atomic labeling scheme (50% probability) of the discrete dimer in **2**.

Description of the Structure 2. Compound **2** is composed of discrete $[Ni(hedpH_2)_2(H_2O)]_2^{4-}$ dimers and pnH_2^{2+} cations. The dimer can be viewed as a fragment of the chain adopted by **1**, which is terminated by the coordination of one molecule of H_2O to each Ni atom (Figure 3). An inversion center sits in the middle of two Ni atoms. Each Ni atom has a distorted octahedral environment with five O atoms from three $hedpH_2^{2-}$ ligands and one O atom from H_2O. The average Ni−O distance 2.066(2) Å agrees well with that of **1**. Two coordination types of $hedpH_2^{2-}$ ligand are found in this dimer. One is bidentate and coordinates to Ni atom as a terminal ligand. The other is tridentate and bridges the two Ni atoms. The P−O(H) bond lengths [1.562(2)−1.579(2) Å] are comparable with those in compound **1**. The coordinated P4−O12 distance [1.488(2) Å], however, is significantly shorter than either the pendant P═O [1.501(2)−1.515(2) Å] or the other coordinated P−O(Ni) [1.505(2)−1.516(2) Å]. The dimers are linked to each other through extensive hydrogen bondings, forming supramolecular networks which is further stabilized by the pnH_2^{2+} cations through hydrogen bondings to the oxygen atoms from both the coordinated water molecules and the phosphonate groups (Figure 4).

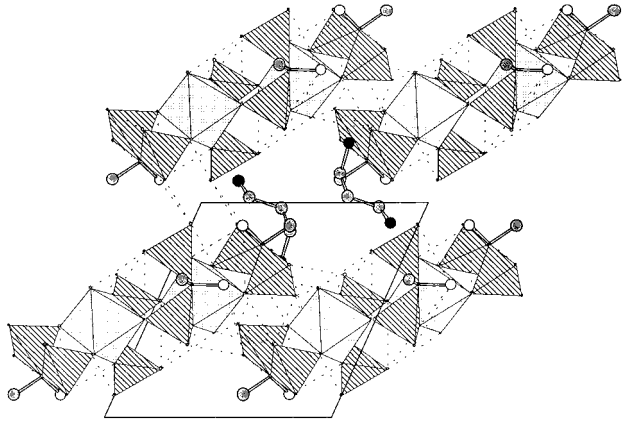

Figure 4. Polyhedral representation of the structure of **2** viewed along *a* axis. All the H atoms and N···hydrogen bondings are omitted for clarity.

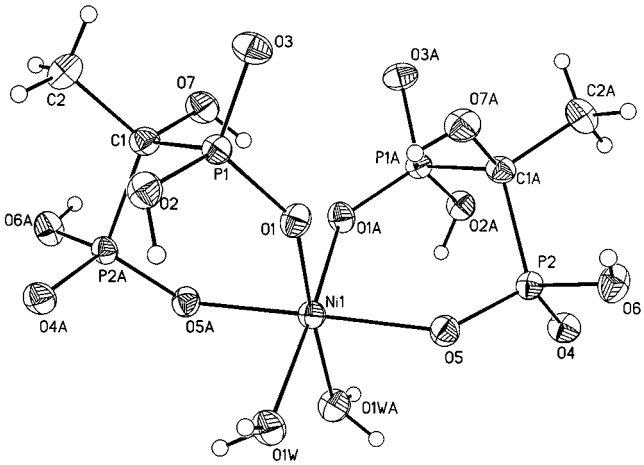

Figure 5. The atomic labeling scheme (50% probability) of the discrete monomer in **3**.

Description of the Structure 3. The compound **3** exhibits a mononuclear structure, different from either **1** or **2**. The Ni atom, sitting in a special position, is coordinated by four O atoms from two equivalent $hedpH_2^{2-}$ ligands and two O atoms from two equivalent water molecules (Figure 5). The geometry around Ni is a slightly distorted octahedral. The average Ni−O distance [2.066(2) Å] agrees well with those in **1** and **2**. The P−O(H) [1.561(2), 1.571(2) Å], P═O [1.502(2), 1.514(2) Å], and P−O(Ni) [1.514(2), 1.518(2) Å] bond lengths are in consistent with those in **1** and **2**. In the lattice, the mononuclear species are hydrogen-bonded to each other, leading to a supramolecular anionic network which is stabilized by bnH_2^{2+} cations through hydrogen bondings (Figure 6).

Template Effect. By employing the ethylenediamine, 1,3-propanediamine, and 1,4-butylenediamine as templates, three new compounds **1**−**3** have been synthesized which exhibit structures that are significantly different from each other, although their formula are similar. In compound **1**, the $\{NiO_6\}$ octahedra and $\{O_3PC\}$ tetrahedra are linked through corner-sharing thus forming one-dimensional chain structure. In compounds **2** and **3**, only discrete dimers $[Ni(hedpH_2)_2(H_2O)]_2^{4-}$ or mononuclear species $[Ni(hedpH_2)(H_2O)_2]^{2-}$ are present.

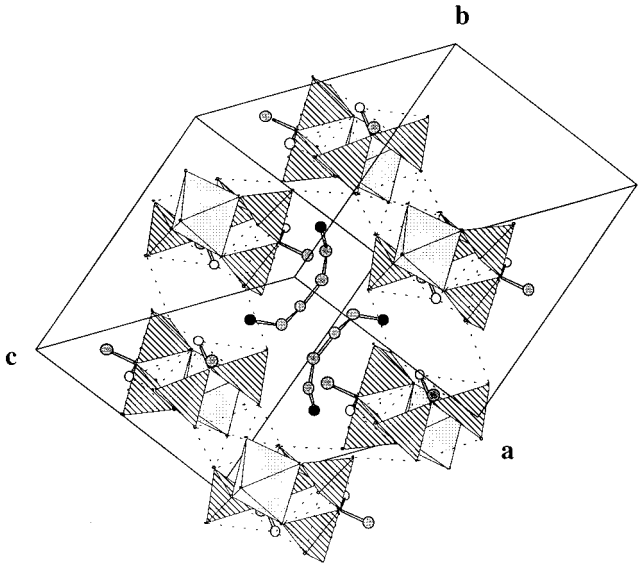

Figure 6. Polyhedral representation of the structure of **3**. All the H atoms and N···hydrogen bondings are omitted for clarity.

The isolation of molecular species such as **2** and **3** by hydrothermal reactions is unexpected. The result reflects, on one hand, the structural diversity on the condensation of nickel octahedra with $hedpH_2^{2-}$ units. On the other hand, since all three compounds were prepared under similar experimental conditions, the templates must play a key role in directing the structures.

In fact, the organic templates used during the preparations of **1**−**3** also serve as charge-compensating cations. Usually, crystal-packing and charge-compensating effects are major determinants of cation incorporation into the solid lattice.[24] A larger cation tends to pack with a larger anion. However, in the present cases, it turns out that the larger cation bnH_2^{2+} prefers to pack with discrete mononuclear anions, whereas the smaller cation enH_2^{2+} directs the formation of a chain compound. From Figures 4 and 6, it is clear that the discrete $[Ni(hedpH_2)_2(H_2O)]_2^{4-}$ dimers in **2** or $[Ni(hedpH_2)(H_2O)_2]^{2-}$ monomers in **3** are efficiently connected to each other, forming three-dimensional frameworks of hydrogen bonding. The cavities generated within the frameworks are filled by protonated 1,3-propanediamine or 1,4-butylenediamine cations. Consequently, the mononuclear species $[Ni(hedpH_2)(H_2O)_2]^{2-}$ may create larger cavities within the hydrogen-bonding frameworks which can hold larger cations. The extensive hydrogen bondings present in the compounds **1**−**3** are, therefore, essential in stabilizing the crystal lattices. The template effect on directing the crystal structures has also been observed in copper(II)−hedp system.[25]

Magnetic Properties. The temperature dependence of the magnetic susceptibility were investigated in the temperature range 280 to 2 K for all three compounds. Figure 7 shows the χ_m and $\chi_m T$ vs T plots for **1**. At 282 K, the observed effective magnetic moment, calculated from $\mu_{eff} = 2.828(\chi_m T)^{1/2}$, is 2.90 μ_B, close to the spin-only value of 2.83 μ_B for a paramagnetic ion of $S = 1$. When the product is cooled from room temperature, the $\chi_m T$ increases slowly and reaches a maximum at 10 K, suggesting a very weak ferromagnetic coupling between the magnetic centers. Below 10 K, the $\chi_m T$ decreases rapidly, which can be due to the zero-field splitting for $S = 1$ species and/or antiferromagnetic exchanges. The susceptibility data were initially analyzed by the expression (1) for a noninteracting ion of $S = 1$ in an axially distorted octahedral surrounding:[21]

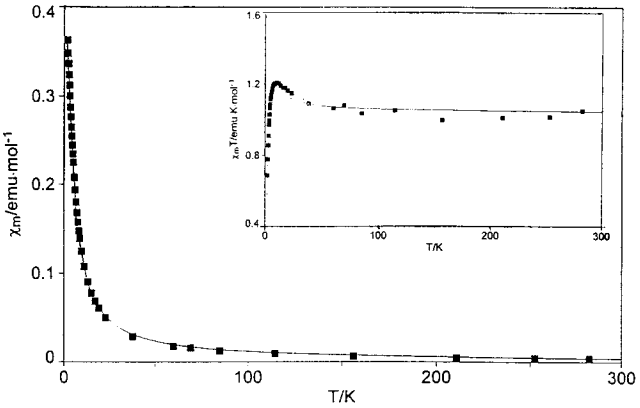

Figure 7. The χ_m and $1/\chi_m$ vs T plots for **1**.

$$\chi_z = \frac{2Ng_z^2\beta^2}{kT}\frac{\exp(-D/kT)}{1+2\exp(-D/kT)}$$

$$\chi_x = \frac{2Ng_x^2\beta^2}{D}\frac{1-\exp(-D/kT)}{1+2\exp(-D/kT)}$$

$$\chi_m = (\chi_z + 2\chi_x)/3 \qquad (1)$$

where N, k, β have their usual meanings. D is the zero-field splitting energy. Assuming $g_x = g_z = g$, the data fit resulted in the parameters $g = 2.25(2)$, $D = 4.67(6)$ cm^{-1}, the coefficient of determination (r^2) 0.999 426 43. The fit is significantly improved, which can be best observed in the $\chi_m T$ vs T curve, when the interaction between the magnetic centers is taken into account:

$$\chi_m' = \chi_m/(1\text{-}zJ'\chi_m)$$

zJ' represents the possible exchanges between Ni(II) centers. The parameters become $g = 2.15(3)$, $D = 5.42(3)$ cm^{-1}, $zJ' = 0.62(6)$ cm^{-1}, $r^2 = 0.999\,858\,73$. The positive zJ' is responsible for a very weak ferromagnetic exchange coupling between the magnetic centers. The susceptibility data were also analyzed on the basis of a chain model for equally spaced centers of $S = 1$.[21] The calculated parameters are $g = 2.42(6)$, $|J| = 0.67(7)$ cm^{-1}, $r^2 = 0.996\,433\,41$.

Clearly, the bulk magnetic behavior of **1** can be well-explained by the single ion expression for $S = 1$ with the inclusion of weak interion exchanges. Such behavior is closely related to its structure. As already described, the structure of **1** is composed of corner-sharing chains of $\{NiO_6\}$ octahedra and $\{O_3PC\}$ tetrahedra. The shortest Ni···Ni distances are 5.257 Å within the chain and

(24) Bonavia, G.; Haushalter, R. C.; O'Connor, C. J.; Zubieta, J. *Inorg. Chem*. **1996**, *35*, 5603.
(25) Zheng, L.-M.; Song, H.-H.; Duan, C.-Y.; Xin, X.-Q. Submitted to *Inorg. Chem*.

8.023 Å between the chains, thus excluding the possible direct exchanges. The superexchange coupling through the O−P−O bridge is very weak because of the electron localization. Therefore, the magnetic behavior of **1** is mainly a single ion behavior with only very weak interion interaction.

The dimer compound **2** and mononuclear species **3** should exhibit similar single ion magnetic behaviors. In contrast to **1**, the $\chi_m T$ value in both cases decreases monotonically upon cooling. On the basis of eq 1, excellent fits were obtained for both compounds. The parameters are $g = 2.09(4)$, $D = 2.80(6)$ cm^{-1}, $r^2 = 0.999\,906\,85$ for **2**, and $g = 2.26(2)$, $D = 0.006$ cm^{-1}, $r^2 = 0.999\,443\,86$ for **3**.

In summary, this paper reports the structures and magnetic properties of three nickel diphosphonates. The structure-directing effect of the organic diamines is remarkable. As far as we are aware, such effect is still not well-documented for the divalent transition metal diphosphonates. We are currently extending this work to the other metal ions. Some interesting results will be reported subsequently.

Acknowledgment. The supports of the National Natural Science Foundation (no. 29823001), the Natural Science Foundation of Jiangsu province (no. BK97018), the State Education Commission, and the Analysis Center of Nanjing University are acknowledged. We also thank Professor K.-H. Lii and Dr. R. Bontchev for the valuable comments and helps.

CM990011V